Pharm Res (2013) 30:1906–1914
DOI 10.1007/s11095-013-1033-4

RESEARCH PAPER

Mapping Ion-Induced Mesophasic Transformation in Lyotropic *In Situ* Gelling System and its Correlation with Pharmaceutical Performance

Sharvil S. Patil • Edakkal Venugopal • Suresh Bhat • Kakasaheb R. Mahadik • Anant R. Paradkar

Received: 8 January 2013 / Accepted: 20 March 2013 / Published online: 18 April 2013

ABSTRACT

Purpose To investigate influence of ion induced mesophasic transformation on pharmaceutical performance of *in situ* gelling system consisting of glyceryl monooleate.

Methods The prepared system showed mesophasic transformation during its conversion from sol to gel upon controlled hydration. The process of mesophasic transformation was studied by SAXS, DSC, rheology and plane polarized light microscopy. Further the influence of additives i.e. naproxen salts (sodium and potassium) and naproxen (base) on the process of mesophasic transformation was also elucidated.

Results It was observed that addition of salt form of naproxen transformed W/O emulsions into cubic mesophase whereas addition of base form of naproxen formed reverse hexagonal (H_{II}) phase upon controlled hydration. The cubic mesophase formed by naproxen salts retarded the drug release for initial 3 h whereas H_{II} phase showed sustained drug release characteristics for naproxen base following Higuchi drug release kinetics.

Conclusion The current work suggests that formulations with tailor made pharmaceutical performance can be developed by selecting proper additives in the system so as to obtain the desired mesophase 'on demand' thereby controlling drug release characteristics.

KEY WORDS cubic phase · hexagonal phase · liquid crystal · mesophasic transformation · sustained drug release

INTRODUCTION

Novel therapeutics generated through the field of nanotechnology requires smart drug delivery systems for attainment of optimum benefits. Lyotropic liquid crystalline phases (LLC) have emerged as one of the drug delivery systems to achieve the said objective. Owing to their structural resemblance to human membranes and large surface area along with high solubilization capacities, LLC can entrap guest molecules with different polarity including biomolecules (1–3). Amphiphilic or polar lipids have been reported to form various lyotropic liquid crystalline phases upon contact with water. The type of liquid crystal (LC) phase formed by the lipid depends on its structural properties, water content and temperature of the system. Small angle X-ray scattering (SAXS), nuclear magnetic resonance (NMR) and optical microscopy have been well reported for characterization of different LC phases formed in lipid/water systems (4). Several research studies on lipid/water systems report occurrence of anisotropic LC phases like lamellar phase, hexagonal phase and transparent cubic phase along with isotropic solutions that contain micelles or vesicles (5–8). The geometrical packing properties of the lipid in particular environment govern the formation of a particular phase (9).

Glycerol monooleate (GMO) is a polar lipid, commonly used as a food emulsifier. It is one of the metabolites obtained after lipolysis of triglycerides (10). It forms a wide variety of LC phases when mixed with water. GMO/water binary system has been well

S. S. Patil · K. R. Mahadik (✉)
Poona College of Pharmacy, Department of Pharmaceutics
Bharati Vidyapeeth Deemed University, Erandwane
Pune 411 038 Maharashtra, India
e-mail: krmahadik@rediffmail.com

S. S. Patil · E. Venugopal · S. Bhat
Polymer Science and Engineering Division
National Chemical Laboratory
Pune 411 008 India

A. R. Paradkar (✉)
Centre for Pharmaceutical Engineering Science
University of Bradford
Bradford, West Yorkshire BD7 1DP, UK
e-mail: A.Paradkar1@bradford.ac.uk

explored which depicts formation of reverse isotropic micellar solution (L2), lamellar (La), inverted type (reverse) hexagonal (H_{II}), and cubic (V2) liquid crystalline phases (11–15). These LC phases have different physical properties and thus have been explored as drug delivery systems including biomolecules. Moreover these LC phases present potential applications in food, pharmaceutical and cosmetic industry (16–21).

Considering the wide applicability of GMO based systems the current work is designed to prepare and characterize drug loaded *in situ* gelling system comprising of GMO, oleic acid and PEG 400. Such system would transform into gel upon controlled hydration. It is believed that such sol to gel transformation may involve formation of different LC phases (mesophases) depending on the structure of additive and the water content. This process is often termed as mesophasic transformation. Recently we have investigated mesophasic transformations involving self emulsification process and its correlation with pharmaceutical performance has been derived (22, 23). Objective of current work is to study and explore the microstructural properties of *in situ* gelling system consisting of GMO and further to investigate the effect of additive on inner structure of the same which is believed to influence the pharmaceutical performance in terms of drug release from the final formulation. The additives used in present work are naproxen salts (sodium and potassium) and naproxen base having different polarities all together.

MATERIALS AND METHODS

Materials

Glyceryl monooleate (GMO, Rylo MG 19 Pharma) was obtained as a gift sample from Danisco culture, Denmark. Oleic acid (OA) and Polyethylene glycol 400 (PEG) were purchased from Loba Chemie Pvt. Ltd, Mumbai and Merck limited, Mumbai, India respectively. Naproxen and Naproxen sodium were generously gifted by Lupin Resaerch Park, Pune. Naproxen potassium was synthesized by dissolving equimolar amount of naproxen and Potassium hydroxide in ethanol under gentle heating (40–45°C). The clear solution thus obtained was filtered through a Whatman filter paper (no. 41) and ethanol was evaporated to obtain a white powder (22).

Methods

Formulation of In Situ Gelling Systems

Different ratios of GMO and OA were screened for *in situ* gelling however it formed stiff gel therefore PEG-400 was incorporated as channel forming agent. The optimized *in situ* gelling system consisted of GMO: OA: PEG in 3:1:1 v/v ratio (PGOP). Naproxen, naproxen sodium and naproxen potassium (0.13 M) each was dissolved in PGOP separately to obtain naproxen loaded PGOP (NGOP), naproxen sodium loaded PGOP (NSGOP) and naproxen potassium loaded PGOP (NKGOP) respectively.

Hydration of In Situ Gelling Systems

The prepared *in situ* gelling systems were hydrated in the range of 5–35% v/v with deionised water and stored for 24 h before analysis.

Characterization

Evaluation of In Situ Gelling Ability

A fixed amount (100 µl) of *in situ* gelling system (PGOP, NGOP, NSGOP and NKGOP) was added to 100 ml distilled water at 25±0.5°C to evaluate their *in situ* gelling ability.

Drug Content

Naproxen and its salt forms from preweighed NGOP, NSGOP and NKGOP respectively were determined by dissolving in 50 ml methanol and recording their absorbance spectrophotometrically at 271 nm.

Rheological Studies

Rheological measurements of intermediate hydrated samples of PGOP, NGOP, NSGOP and NKGOP were performed using a controlled stress rheometer (Viscotech Rheometer, Rheologica Instruments AB, Lund, Sweden). Data analysis was done with Stress RheoLogic Basic software, version 5.0. A cone and plate geometry was used with 25 mm diameter and cone of 1.0 °. The measurements were carried out on the controlled hydrated samples after 24 h of hydration at 25±0.5°C (24). Viscometry and creep recovery tests were performed in triplicate on intermediate hydrated samples of PGOP, NGOP, NSGOP and NKGOP.

Viscometry. Intermediate hydrated samples (5–35%v/v) of PGOP, NGOP, NSGOP and NKGOP with shear stress varying in the range of 0.1–50 Pa.

Creep-Recovery. Samples were subjected to a constant stress of 1 Pa (as determined from Linear Viscoelastic Region) for 100 s followed by recovery of sample for 200 s. The creep compliance, J (defined as ratio between measured strain and applied stress) was recorded against time. Percent

creep recovery was calculated by using the formula given below.

$$\delta J = \left\{ \frac{J(100s) - J(300s)}{J(100s)} \right\} \times 100 \quad (1)$$

where $J(100\ s) = J$ value at 100 s and $J(300\ s) = J$ value at 300 s

Polarized Light Microscopy

Polarized light microscopy of hydrated *in situ* gelling system was performed for identifying the type of mesophase formed in the prepared sample (25). Hydrated *in situ* gelling system (PGOP, NGOP, NSGOP and NKGOP) was transferred to a specially fabricated glass tube (internal diameter 0. 5 cm) and viewed for presence or absence of birefringence under a microscope at 25±0.5°C with a λ/4 plate oriented at 45° to the polarizer axes under 40X magnification (Nikon Eclipse E 600, Nikon Instech Co., Japan).

Small Angle X-ray Scattering (SAXS) Studies

Small angle X-ray scattering experiments were done on a Bruker Nanostar with rotating Cu anode and pinhole geometry. The instrument uses a copper Kα radiation of wavelength 1.54 Å. The anode was operated with a current of 100 mA and a potential difference of 45 kV, and the sample to detector distance was 105 cm. The samples were taken in a quartz capillary of 2 mm diameter and 10 μm wall thickness. Background from an empty capillary was subtracted, after accounting for the sample absorption. A Bruker Peltier heating cooling unit was used for temperature control in the system. The data was collected on a HISTAR gas-filled multiwire detector and was circularly averaged to get a 1D curve. The scattering from intermediate hydrated samples of PGOP, NSGOP, NKGOP and NGOP was measured for long enough that the scattered intensity gave at least 3 million counts on the detector.

Differential Scanning Calorimetry (DSC)

Calorimetric measurements were performed with Mettler Toledo 821e instrument equipped with an intracooler (Mettler Toledo, Switzerland), and calibrated with indium and zinc standards. 10±3 mg of 15% v/v hydrated PGOP, NSGOP, NKGOP and NGOP sample was placed in aluminum crucibles which were hermetically sealed. The crucibles were then cooled to −25°C at the rate of 10°C/min. and maintained at −25°C for 10 min. The crucibles were then subjected to heating from −25°C to 5°C at the scanning rate of 3°C/min.

In Vitro Drug Diffusion Studies

In vitro drug diffusion studies were carried out for NGOP, NKGOP and NSGOP using dialysis technique in triplicate. One end of pretreated cellulose dialysis tubing (7 cm in length) having molecular cut off (pore size) of 12,400 Da was tied with thread and then 1 ml of NGOP (equivalent to 30 mg naproxen) was placed in it along with 5 ml of dialyzing medium (distilled water). The other end of tubing was also secured with thread and was allowed to rotate freely in dissolution vessel of USP 24 type II dissolution test apparatus that contained 900 ml dialyzing media (distilled water) maintained at 37±0.5°C and stirred at 100 rpm. Placebo formulation (PGOP) was also tested likewise simultaneously under identical conditions so as to check interference, if any. Aliquots were collected periodically and replaced with fresh dialyzing medium. Aliquots, after filtration through Whatman filter paper (no. 41), were analyzed spectrophotometrically at 271 nm for naproxen content. Similar procedure was followed for *in vitro* drug diffusion study of NSGOP, NKGOP, naproxen, naproxen salts (sodium and potassium) alone. The data was analyzed using PCP Disso v 3i software.

Estimation of Distribution Coefficient

The distribution of naproxen and its salts between the mesophase and the aqueous phase at equilibrium was determined experimentally as partition coefficient (P). A known amount of naproxen (0.01 M) was dissolved in PGOP and equal volume of water was added to this mixture. The system thus obtained was shaken for 4 days at 25±0.5°C (26). The aliquots of water was removed from the system and analyzed spectrophotometrically at 271 nm for naproxen content. The amount of naproxen in both the phases was obtained by mass balance equation. The partition coefficient was calculated.

The distribution coefficient was calculated from the formula

$$\log D_{l/w} = \log P + \log \left[\frac{1}{1 + 10^{(pH - pKa)}} \right]$$

where $\log D_{l/w}$ = distribution coefficient between mesophase (lipid) and water

The pH of the system was about 7. The analysis was done in triplicate. Similar procedure was used for determination of distribution coefficient of naproxen sodium and naproxen potassium.

RESULTS AND DISCUSSION

The preliminary studies showed formation of stiff gel upon hydration of different ratios of GMO and OA which

released negligible amount of drug even after 7–8 h. Hence PEG 400 was introduced into the mixture of GMO and OA as a channel forming agent. The addition of PEG 400 modulated the gel appearance upon hydration along with the drug release profiles of the prepared systems. Different hydration levels were required for different samples for their transformation into gel. NSGOP transformed into gel after addition of 25%v/v of water whereas PGOP and NKGOP required 30%v/v of water for transformation into gel. However, 35%v/v of water was required for transformation of NGOP into gel. To investigate this further inner structure of all the prepared samples were studied by plane polarized light microscopy, SAXS, DSC and rheology.

Plane Polarized Light Microscopy

The intermediate hydration regimes of all the prepared samples before its transformation into gel showed formation of W/O emulsion. NSGOP and NKGOP formed clear transparent gel upon hydration which did not show any birefringence indicating formation of cubic mesophase. However, PGOP and NGOP showed birefringence with fan like structures upon complete sol to gel transformation. The formation of fan like structures in PGOP and NGOP gel samples suggested conversion of W/O emulsion into H_{II} phase (Fig. 1) (25).

Small Angle X-ray Scattering (SAXS)

There are reports stating utility of SAXS for investigation of microstructure of colloidal systems (27, 28). The extent of microstructural alterations induced in the drug loaded *in situ* gelling system when compared to PGOP was investigated by using SAXS. Figure 2 depicts the SAXS patterns of prepared samples.

PGOP, NGOP, NSGOP and NKGOP systems formed W/O emulsion at lower hydration levels (20% v/v) which

Fig. 1 Polarized optical microscope image of Reverse Hexagonal phase.

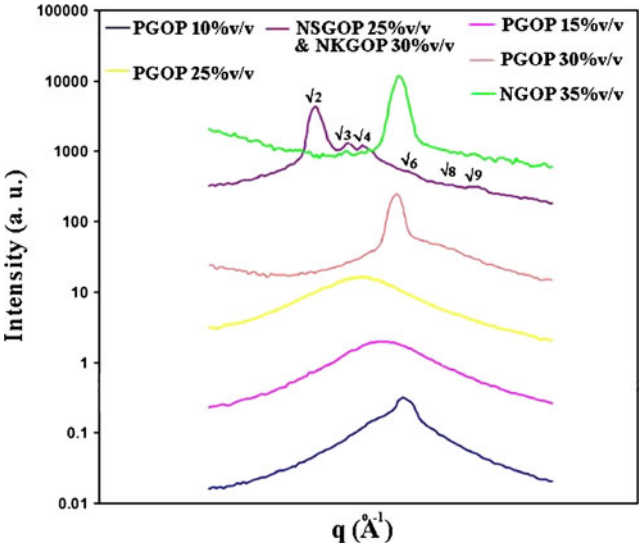

Fig. 2 Representative SAXS patterns of prepared samples at different hydration levels.

transformed into gel with further hydration. It was observed that before transformation of W/O emulsion into gel all the prepared samples showed broad peak. However, upon complete transformation into gel after hydration the SAXS pattern for NSGOP, NKGOP was markedly different when compared to PGOP and NGOP. NSGOP and NKGOP indicated cubic mesophase formation whereas PGOP and NGOP formed H_{II} mesophase upon complete transformation into gel. Moreover the cubic phase formed by NSGOP and NKGOP was Pn3m (double diamond type) with peak spacing in the ratio of √2: √3: √4: √6: √8: √9 (21). This supported our readings of plane polarized light microscopy and confirmed different mesophases formation in case of samples containing naproxen salts (NSGOP and NKGOP) as compared to that of sample containing naproxen base (NGOP). According to the Hofmeister series ions can be classified as salting out ions and salting in ions. Salting out ions, also called kosmotropic ions or water structure makers, are usually small and have relatively low polarizability, have high electric fields at short distances and lose their water of hydration with great difficulty. Salting in ions, also called chaotropic ions or water structure breakers, have the opposite characteristics. Naproxen sodium solute is kosmotropic while the behavior of potassium ions is chaotropic (29–32). The rapid sol–gel transformation (i.e. at lower hydration level) shown by NSGOP when compared to other samples may be attributed to the hydration of GMO and PEG chains owing to kosmotropic activity of sodium ions. However, in case of NKGOP the hydration of GMO and PEG chains was hindered by the combined water repellant activity of oleic acid and potassium ions (chaotropic activity). Thus NKGOP required more water for sol–gel transformation when compared to NSGOP. NGOP required highest hydration among all the

samples for sol–gel transformation which may be attributed to dehydration of GMO headgroups induced by hydrophobic naproxen owing to its high log *P* value (3.22) along with hydrophobic oleic acid as well.

The formation of H_{II} phase upon addition of oleic acid to GMO has been well reported (33). The presence of oleic acid in the system increases apparent hydrophobic volume of the lipid which ultimately increases the critical packing parameter by relaxing the alkyl chain packing stress. This results in a transition of W/O emulsion to H_{II} phase. In case of NGOP, presence of naproxen further increased the apparent hydrophobic volume which thus transformed into H_{II} phase. However the ions associated with NSGOP and NKGOP might have migrated to water phase and therefore the systems could not achieve the CPP values required for hexagonal symmetry thus forming cubic mesophase. Yet another reason responsible for the formation of cubic phase by NSGOP and NKGOP may be associated with the screening of electric potential of OA/GMO/PEG membrane by the ions (sodium and potassium) through electrostatic interactions with GMO headgroups (34). The results of SAXS were further supported by DSC and rheology.

Differential Scanning Calorimetry

Considering the fact that microstructural changes taking place during *in situ* gelling process may alter thermodynamic property of water, the intermediate hydrated systems were analyzed by subzero temperature differential scanning calorimetry. The position of endothermic peak observed for water in DSC thermogram provides information about the nature of water. Depending on the peak position, water can be bound (which is associated to hydrophilic groups and melts below −10°C), interphasal water (defined as water confined within the interface of dispersed system, which melts at about −10°C) or free water which melts at ~0°C (35, 36). Figure 3 shows DSC thermogram of water and intermediate hydrated sample (15%v/v) of PGOP, NSGOP, NKGOP and NGOP. The DSC thermogram of water showed an exothermic peak at about −8°C due to crystallization of water and a melting endotherm at about 0°C representing water melting. The endothermic peak observed for water in all the samples (except NGOP) was about −2°C confirming that it is interphasal water. Moreover, PGOP, NGOP and NKGOP showed endothermic peak at about 0°C corresponding to free water. All the samples showed an exothermic peak at about −15°C representing crystallization of GMO as confirmed from DSC thermogram of hydrated (15%v/v) GMO alone (Fig. 3). The endothermic events observed in DSC studies are listed in Table I.

The degree of binding strength of water with the surfactants and drug molecules was determined from the fusion temperatures and enthalpies of interphasal water as analyzed

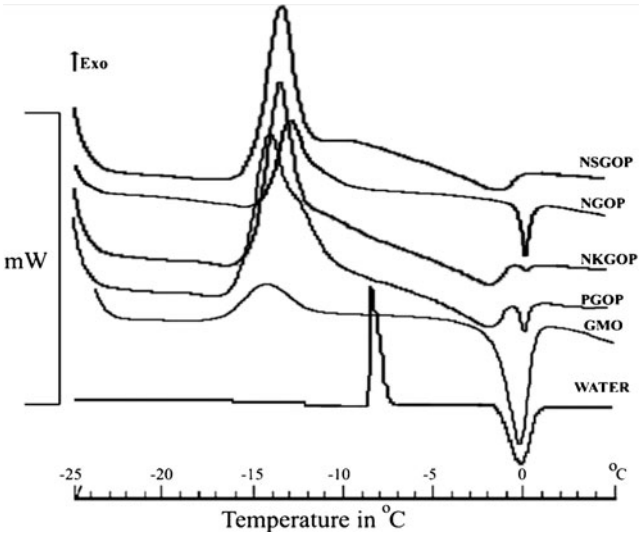

Fig. 3 DSC thermogram of water and intermediate hydrated sample (15%v/v) of GMO, PGOP, NSGOP, NKGOP and NGOP.

by DSC (37). PGOP and NSGOP showed endothermic peak at −2.37°C and −2.39°C with enthalpies −4.54 Jg^{-1} and −1.27 Jg^{-1} respectively. Thus it was observed that introduction of naproxen sodium into PGOP significantly increased enthalpy (around 72%) indicating that the thermodynamic properties of water associated with GMO and PEG chains at the interface was significantly altered. This may be due to stronger binding of water molecules to surfactants and sodium ions at the interface. The presence of free water in case of PGOP as evident from DSC thermogram may be attributed to water repellant activity of oleic acid which might have interfered with the binding of water molecules to surfactant chains.

The comparison of endothermic events of NKGOP with PGOP suggested increase in enthalpy of NKGOP (around 42%) suggesting binding of water molecules to the surfactant chains. Moreover, NKGOP also showed presence of free water within system which may be attributed to combined water repellant effect of oleic acid (hydrophobic nature) and potassium ions (chaotropic activity) present within NKGOP. This might have resulted in disruption of water structure at the interface.

DSC thermogram of NGOP showed only free water peak suggesting that the binding of water molecules with surfactant chains was strongly hindered. Such hindrance to the binding of water molecules to surfactant may be attributed to the combined hydrophobic activity of naproxen (log P=3.22) and oleic acid. In other words the results of DSC studies indirectly focused on the gel formation process which involves hydration of surfactant chains. Thus NGOP suggested prolongation of *in situ* gelling process when compared to other samples. The results of DSC were further supported by rheological analysis of the intermediate hydrations.

Table I Thermal Behavior of Systems at 15%v/v Dilution with Water

Sr. No.	Sample	Endothermic peak temperature (°C)		Enthalpy (Jg^{-1})	
		Interphasal water	Free water	Interphasal water	Free water
1	PGOP	−2.37	0	−4.54	−1.38
2	NSGOP	−2.39	–	−1.27	–
3	NGOP	–	−0.014	–	−7.79
4	NKGOP	−2.44	−0.17	−2.63	−0.21

Rheology

Rheological properties of material are a function of both the structural arrangement of particles and interparticle forces. Hence, in the present work microstructural analysis of intermediate hydrated regimes was performed using viscometry and creep recovery studies. The plot of shearing stress *versus* shear rate for all the samples from intermediate hydration regime was linear suggesting Newtonian flow associated with them (not shown). Figure 4 shows plot of viscosity *versus* hydration (% v/v of water) for intermediate regimes of PGOP, NGOP, NSGOP and NKGOP. The increasing viscosity of the intermediate hydrated regimes with successive hydration supported the results probed by SAXS and DSC. The reports state that progressive hydration of surfactant headgroups enhances their mobility as analyzed by NMR. This entropy driven process leads to progressive loosening-up of the headgroup packing which in turn might have raised the viscosity of the system (38, 39). Moreover, such increase in viscosity confirmed sol to gel transformation within the system with controlled hydration. The order in which reduction in viscosity was observed can be represented as NSGOP> PGOP>NKGOP>NGOP.

The highest viscosity associated with NSGOP may be attributed to the kosmotropic effect of sodium ions which lead to hydration of surfactant chains. The viscosity of intermediate hydrations of NKGOP was lower when compared to PGOP. The combined water repellant activity of potassium ion and oleic acid might have been responsible for such change as explained previously. NGOP samples showed lowest viscosity when compared to other samples suggesting that hydration of surfactant chains was hindered by the hydrophobic nature of naproxen and oleic acid. To confirm the results of viscometry studies we analyzed the samples by creep recovery test.

The elastic character present within system can be readily depicted by Creep recovery test (40). The percent creep value is directly proportional to elastic component present within system. Higher the value of creep more will be elastic component present within the system. Figure 5 shows creep recovery curves for all the prepared samples.

The curves were recorded for all the samples upon their transformation into gel. Table II shows percent creep recovery data for the prepared gels. It was observed that sol to gel transformation was fastest in case of NSGOP whereas it was slowest for NGOP. Hydration of surfactants played

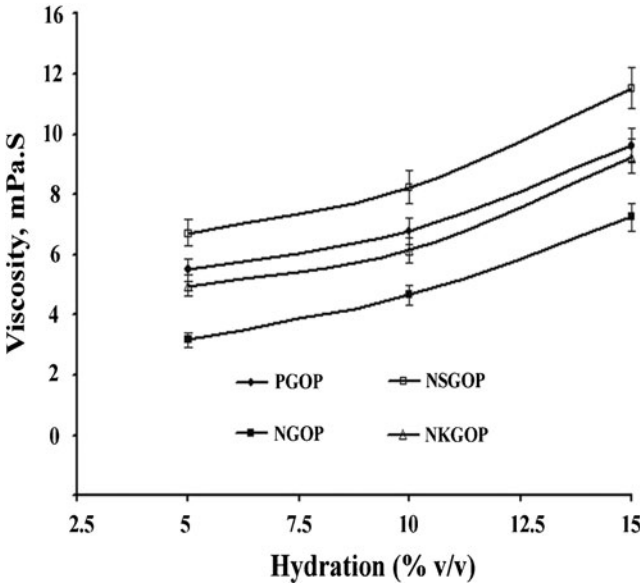

Fig. 4 Plot of viscosity *versus* hydration (% v/v) for intermediate regimes of PGOP, NSGOP, NKGOP and NGOP ($n=3$).

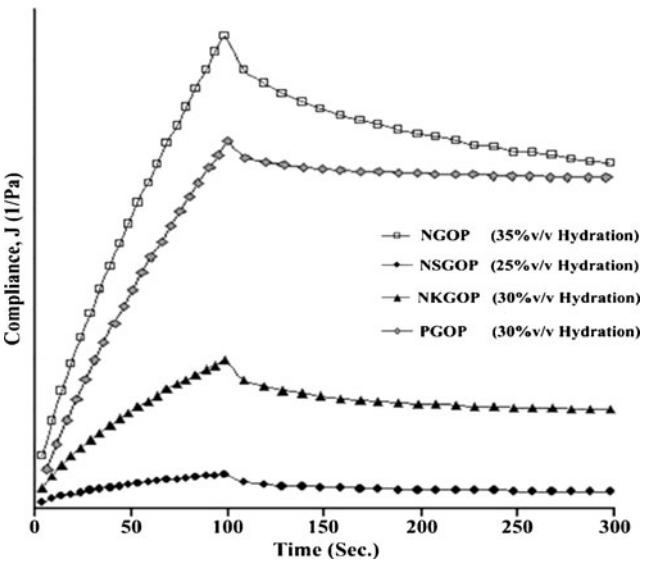

Fig. 5 Representative graph of Creep recovery test for the prepared *in situ* gels of PGOP, NSGOP, NKGOP and NGOP.

Table II Percent Creep Recovery for All the Samples After Transformation into Gel

Sample	Hydration (% v/v)	Percent Creep recovery
PGOP	30	18.19 ± 1.907
NSGOP	25	9.84 ± 2.394
NGOP	35	32.486 ± 3.03
NKGOP	30	26.336 ± 2.96

Mean ± SD, $n = 3$

crucial role in sol–gel transformation. The gel formed in case of NSGOP had creep value of 9.84 ± 2.394%. The reason for lower elastic component of NSGOP may be attributed to the kosmotropic effect of sodium ions which lead to effective hydration of surfactant chains through hydrogen bonding of water molecules. Such hydrogen bonding with surfactant chains might have decreased their flexibility. However, the creep value associated with NGOP was 32.486 ± 3.03% suggesting higher elastic component associated with it. The combined hydrophobic effect of naproxen and oleic acid might have hindered with the hydrogen bonding of water molecules with surfactant chains, thus keeping their flexibility intact when compared to other samples. In case of NKGOP the chaotropic effect of potassium ions along with hydrophobic oleic acid prevented hydration of surfactant chains keeping their flexibility intact. Thus NKGOP showed higher creep value when compared to PGOP. The results of rheology were in agreement with the DSC results.

In Vitro Drug Release Study

The drug release from lyotropic liquid crystals have been shown to be governed by the type of mesophase formed upon hydration of the system (41). The present work highlights effect of additive on microstructure of *in situ* gelling system which in turn governs the drug release kinetics of the prepared system. Thus *in vitro* drug release study can be used as a tool to assess the performance of prepared gel formulations.

Drug release study for the samples containing naproxen salts and naproxen base was performed in distilled water. Samples containing salt forms of naproxen (NSGOP and NKGOP) retarded the drug release for initial 3 h when compared to dissolution profiles of naproxen sodium and naproxen potassium alone (Fig. 6). Moreover the percent of naproxen potassium released from NKGOP was more for initial 1 h when compared to NSGOP which eventually became comparable after 2 h. Such behavior may be attributed to the rapid transformation of NSGOP into cubic gel as compared to NKGOP owing to kosmotropic activity of sodium ions. Dispersion of formed microstructures into the

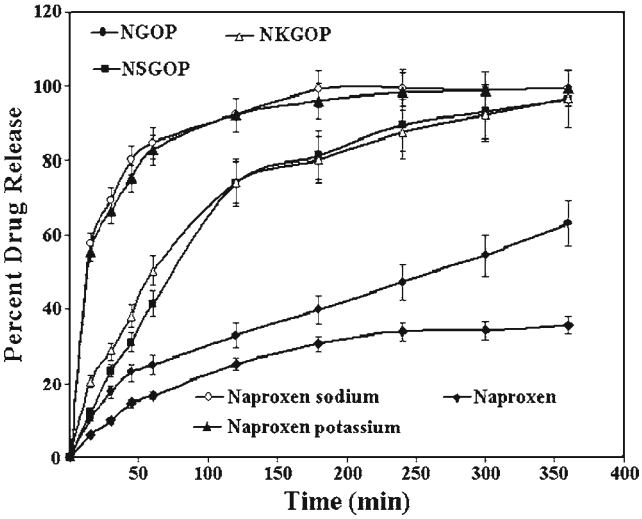

Fig. 6 *In vitro* drug release profiles of NGOP, NSGOP, NKGOP, naproxen, naproxen sodium and naproxen potassium ($n = 3$).

dissolution medium might have resulted in the similar drug release profiles for NKGOP and NSGOP after 2 h. Naproxen salts transformed into gel with cubic microstructure whereas naproxen base retained the H_{II} structure upon transformation into gel.

The dissolution data of NGOP showed sustained drug release following Higuchi drug release kinetics. The drug release kinetics indicated encapsulation of drug within the hexagonal structure of the gel matrix which showed linear drug release as a function of square root of time. In the case of the H_{II} phase, the aqueous compartments are closed extended micellar columnar structures and the lipophilic drugs will be located within the lipid domain and amphiphilic drugs at the interface. Thus naproxen base is released faster from H_{II} phase. Moreover the presence of hydrophilic PEG molecules within NGOP might have improved the dissolution rate of hydrophobic naproxen as compared to dissolution rate of naproxen base alone. This was further investigated by determining the distribution coefficient of naproxen and its salts between mesophase and water. Distribution co-efficient (log D) of naproxen sodium and naproxen potassium was found to be -0.3831 ± 0.01 and -0.409 ± 0.14 respectively. There was no significant difference ($p < 0.05$) in the value of distribution coefficient of naproxen salts when analyzed statistically (Tukeys test) indicating that the molar concentration of naproxen ion was similar when equilibrium was achieved in the prepared system. This is in accordance with the dissolution profiles of NKGOP and NSGOP since their drug release profiles were observed to be comparable after 3 h. The distribution coefficient of naproxen between hexagonal phase and water was found to be 0.445 ± 0.011. The distribution coefficient of naproxen suggested that the molar concentration of naproxen was higher in hexagonal phase when compared

to water. Thus to conclude, H_{II} phase showed sustained drug release characteristics for naproxen base whereas *in situ* cubic mesophase formed by naproxen salts retarded the drug release for initial 3 h.

CONCLUSION

The present work explores inner structure of intermediate hydration regimes of the prepared *in situ* gelling system and its alteration by the addition of guest molecule (drug) which in turn changes the type of mesophase formed by the prepared system. The hydrophobic additives formed H_{II} phase whereas naproxen salts formed cubic mesophase upon hydration of the system which ultimately influenced the drug release characteristics. The cubic mesophase formed by naproxen salts retarded the drug release for initial 3 h whereas H_{II} phase showed sustained drug release characteristics for naproxen base following Higuchi drug release kinetics. Thus to conclude, the current work emphasizes the fact that formulations with tailor made pharmaceutical performance can be developed by selecting proper additives in the system so as to obtain the desired mesophase 'on demand' thereby controlling the drug release characteristics.

ACKNOWLEDGMENTS AND DISCLOSURES

The authors thank Dr. Guruswamy Kumaraswamy, Scientist, Polymer Chemistry, National Chemical Laboratory, Pune for providing facility of Small Angle X ray Scattering and for extending his cooperation in SAXS data analysis and discussion.

REFERENCES

1. Fahr A, van Hoogevest P, May S, Bergstrand N, Leigh M. Transfer of lipophilic drugs between liposomal membranes and biological interfaces: consequences for drug delivery. Eur J Pharm Sci. 2005;26:251–65.
2. Shan-Yang L, Hsiu-Li L, Mei-Jane L. Adsorption of binary liquid crystals onto cellulose membrane for thermo-responsive drug delivery. Adsorption. 2002;8:197–202.
3. Jensen J, Schutzbach J. Activation of mannosyltransferase II by nonbilayer phospholipids. Biochemistry. 1984;23:1115–9.
4. Caboi F, Nylander T, Razumas V, Talaikyte Z, Monduzzi M, Larsson K. Structural effects, mobility, and redox behavior of vitamin K1 hosted in the monoolein/water liquid crystalline phases. Langmuir. 1997;13:5476–83.
5. Lindblom G, Rilfors L. Cubic phases and isotropic structures formed by membrane lipids—possible biological relevance. Biochim Biophys Acta. 1989;988:221–56.
6. Larsson K. Cubic lipid-water phases: structures and biomembrane aspects. J Phys Chem. 1989;93:7304–14.
7. Seddon J. Lyotropic phase behaviour of biological amphiphiles. Ber Bunsenges Phys Chem. 1996;100:380–93.
8. Chang C, Bodmeier R. Effect of dissolution media and additives on the drug release from cubic phase delivery systems. J Control Release. 1997;46:215–22.
9. Isrealachvilli J, Mitchell D, Ninham B. Theory of self-assembly of hydrocarbon amphiphiles into micelles and bilayers. J Chem Soc Faraday Trans II. 1976;72:1525–68.
10. Patton J, Carey M. Watching fat digestion. Science. 1979;204:145–8.
11. Chernik G. Phase studies of surfactant-water systems. Curr Opin Colloid Interface Sci. 2000;4:381–90.
12. Larsson K. Two cubic phases in monoolein/water system. Nature. 1983;304:664.
13. Lutton E. Phase behavior of aqueous systems of monoglycerides. JAOCS. 1965;42:1068–70.
14. Qiu H, Caffrey M. The phase diagram of the monoolein/water system: metastability and equilibrium aspects. Biomaterials. 2000;21:223–34.
15. Rappolt M, Di Gregorio G, Almgren M, Amenitsch H, Pabst G. Non-equilibrium formation of the cubic Pn3m phase in a monoolein/water system. Europhy Lett. 2006;75:267–73.
16. Drummond C, Fong C. Surfactant self-assembly objects as novel drug delivery vehicles. Curr Opin Colloid Interface Sci. 2000;4:449–56.
17. Caboi F, Murgia S, Monduzzi M, Lazzari P. NMR investigation on Melaleuca Alternifolia essential oil dispersed in the monoolein aqueous system: phase behavior and dynamics. Langmuir. 2002;18:7916–22.
18. Shah M, Paradkar A. Cubic liquid crystalline glyceryl monooleate matrices for oral delivery of enzyme. Int J Pharm. 2005;294(1–2):161–71.
19. Sadhale Y, Shah J. Glyceryl monooleate cubic phase gel as chemical stability enhancer of cefazolin and cefuroxime. Pharm Dev Tech. 1998;3(4):549–56.
20. Fong W, Hanley T, Boyd B. Stimuli responsive liquid crystals provide 'on-demand' drug delivery *in vitro* and *in vivo*. J Control Rel. 2009;135(3):218–26.
21. Yaghmur A, Laggner P, Zhang S, Rappolt M. Tuning curvature and stability of monoolein bilayers by designer lipid-like peptide surfactants. PLoS One. 2007;2(5):e479.
22. Patil S, Venugopal E, Bhat S, Mahadik K, Paradkar A. Probing influence of mesophasic transformation in self-emulsifying system: effect of ion. Mol Pharm. 2012;9(2):318–24.
23. Patil S, Venugopal E, Bhat S, Mahadik K, Paradkar A. Microstructural elucidation of self-emulsifying system: effect of chemical structure. Pharm Res. 2012;29:2180–8.
24. Biradar S, Dhumal R, Paradkar A. Rheological investigation of self-emulsification process. J Pharm Pharm Sci. 2009;12(1):17–31.
25. Rosevear F. The microscopy of the liquid crystalline neat and middle phases of soaps and synthetic detergents. J Am Oil Chem Soc. 1954;31:628–39.
26. Clogston J, Craciun G, Hart D, Caffrey M. Controlling release from the lipidic cubic phase by selective alkylation. J Control Release. 2005;102:441–61.
27. Glatter O, Orthaber D, Stradner A, Scherf G, Fanun M, Garti N, *et al.* Sugar-Ester nonionic microemulsion :structural characterization. J Colloid Interface Sci. 2001;241:215–25.
28. Salonen A, Muller F, Glatter O. Dispersions of internally liquid crystalline systems stabilized by charged disklike particles as pickering emulsions: basic properties and time-resolved behavior. Langmuir. 2008;24(10):5306–14.
29. Yariv D, Efrat R, Libster D, Aserin A, Garti N. *In vitro* permeation of diclofenac salts from lyotropic liquid crystalline systems. Colloid Surfaces B. 2010;78:185–92.
30. Collins K, Washabaugh M. The Hofmeister effect and the behaviour of water at interfaces. Q Rev Biophys. 1985;18(4):323–422.
31. Cacace M, Landau E, Ramsden J. The Hofmeister series: salt and solvent effects on interfacial phenomena. Q Rev Biophys. 1997;30:241–77.

32. Dong R, Hao J. Complex fluids of Polyoxyethylene Monoalkyl Ether nonionic surfactants. Chem Rev. 2010;110:4978–5022.
33. Borne J, Nylander T, Khan A. Phase behavior and aggregate formation for the aqueous monoolein system mixed with sodium oleate and oleic acid. Langmuir. 2001;17:7742–51.
34. Li S, Yamashita Y, Yamazaki M. Effect of Electrostatic Interactions on Phase Stability of Cubic Phases of Membranes of Monoolein/ Dioleoylphosphatidic Acid Mixtures. Biophys J. 2001;81:983–93.
35. Senatra D, Lendinara L, Giri M. W/O microemulsions as model systems for the study of water confined in microenvironments: low resolution 1H magnetic resonance relaxation analysis. Prog Colloid Polym Sci. 1991;84:122–8.
36. Schulz P, Puig J, Barreiro G, Torres L. Thermal transitions in surfactant-based lyotropic liquid crystals. Thermochim Acta. 1994;231:239–56.
37. Kogan A, Shalev D, Raviv U, Aserin A, Garti N. Formation and Characterization of ordered bicontinuous microemulsions. J Phys Chem B. 2009;113:10669–78.
38. Ulrich A, Watts A. Molecular response of the lipid headgroup to bilayer hydration monitored by 2H-NMR. Biophys J. 1994;66:1441–9.
39. Mezzenga R, Meyer C, Servais C, Romoscanu A, Sagalowicz L, Hayward R. Shear rheology of Lyotropic liquid crystals: a case study. Langmuir. 2005;21(8):3322–33.
40. Tadros T. Application of rheology for assessment and prediction of the long-term physical stability of emulsions. Adv Colloid Interface. 2007;109:227–58.
41. Negrini R, Mezzenga R. pH-responsive lyotropic liquid crystals for controlled drug delivery. Langmuir. 2011;27:5296–303.